

## Substitution Reactions on Cyclometalated Pt(IV) Complexes. Associative Tuning by Fluoro Ligands and Fluorinated Substituents

Paul V. Bernhardt,<sup>†</sup> Carlos Gallego,<sup>‡</sup> Manuel Martinez,<sup>\*,‡</sup> and Teodor Parella<sup>§</sup>

Department of Chemistry, University of Queensland, Brisbane 4072, Australia, Departament de Química Inorgànica, Universitat de Barcelona, Martí i Franquès 1-11, E-08028 Barcelona, Spain, and Servei de Ressonància Magnètica Nuclear, Universitat Autònoma de Barcelona, E-08193 Bellaterra, Spain

Received July 30, 2001

The substitution reactions of sulfide by phosphines on Pt(IV) complexes having a cyclometalated imine ligand, two methyl groups in a *cis* geometrical arrangement, and a halogen and a sulfide as ligands, [Pt (Me)<sub>2</sub>X(C<sup>∧</sup>N)(SR<sub>2</sub>)], have been studied as a function of temperature, solvent, and electronic and steric characteristics of the phosphines, sulfides, X, and C<sup>∧</sup>N. In most of these cases, a limiting dissociative mechanism has been found, where the dissociation of the sulfide ligand corresponds to the rate-determining step. The intermediate species formed behaves as a true pentacoordinated Pt(IV) compound in a steady-state concentration only for the systems with SME<sub>2</sub>; for the bulkier SEt<sub>2</sub> and SBzI<sub>2</sub> leaving ligands the rate constants and activation parameters show an important degree of solvent dependence, which correlates with the ability of the solvent to form hydrogen bonds. The X-ray crystal structure of one of the dibenzyl sulfide complexes has been determined, and the geometrical arrangement of the ligands has been determined by NOE NMR measurements at low temperature. The nature of the solvent, imine, sulfide, and halogen ligands produces differences in the reaction rates, which can be quantified very well by the corresponding  $\Delta S^\ddagger$  values that move from +48 to -90 J K<sup>-1</sup> mol<sup>-1</sup>. The reaction on [Pt(Me)<sub>2</sub>F(C<sub>5</sub>CF<sub>4</sub>CHNCH<sub>2</sub>Ph)(SME<sub>2</sub>)] has been found to take place via a mechanism that depends strongly on the bulkiness of the substituting phosphine. While for PCy<sub>3</sub> the reaction is dissociative, for smaller entering ligands the first associatively activated substitution mechanisms on organometallic Pt(IV) complexes have been established with values of  $\Delta H^\ddagger$  and  $\Delta S^\ddagger$  in the 28–44 kJ mol<sup>-1</sup> and -120 to -83 J K<sup>-1</sup> mol<sup>-1</sup> ranges. Important intramolecular hydrogen bonding in the starting material can be held responsible for this difference with the remaining systems.

### Introduction

Low-spin octahedral t<sub>2g</sub><sup>6</sup> complexes are considered as having a definite inert character with respect to their substitution reactions.<sup>1</sup> Although octahedral Pt(IV) complexes are a clear candidate for the study of the degree of associativeness/dissociativeness of these substitution processes given their extreme inertness, the presence minute quantities of Pt(II) complexes that catalyze the reactions via substitution

reactions that have a clear associative character<sup>2</sup> have prevented its proper study and mechanistic assignment. The introduction of an important number of C–M bonds in any complex seems to produce an important degree of dissociativeness, due to the important *trans* influence of these C–M bonds.<sup>3</sup> Furthermore, the introduction of very good  $\sigma$  donors on the coordination sphere should lead to an increase in the metal electron density that could produce an increase of its lability.<sup>4</sup> Consequently, it is not strange that the introduction of Pt–C bonds in Pt(IV) t<sub>2g</sub><sup>6</sup> complexes leads to an important

\* To whom correspondence should be addressed. E-mail: manel.martinez@qi.ub.es.

<sup>†</sup> University of Queensland.

<sup>‡</sup> Universitat de Barcelona.

<sup>§</sup> Universitat Autònoma de Barcelona.

(1) (a) Tobe, M. L.; Burgess, J. *Inorganic Reaction Mechanisms*; Longman: Harlow, U.K., 1999. (b) Dixon, N. E.; Lawrance, G. A.; Lay, P. A.; Sargeson, A. M. *Inorg. Chem.* **1983**, *22*, 846. (c) Curtis, N. J.; Lawrance, G. A.; Lay, P. A.; Sargeson, A. M. *Inorg. Chem.* **1986**, *25*, 484.

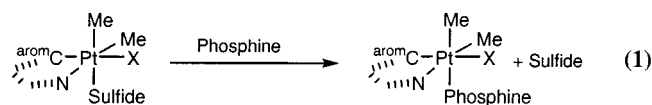
(2) (a) Peloso, A. *Coord. Chem. Rev.* **1973**, *10*, 123. (b) Dixon, N. E.; Lawrance, G. A.; Lay, P. A.; Sargeson, A. M. *Inorg. Chem.* **1984**, *23*, 2940. (c) Drouge, L.; Elding, L. I. *Inorg. Chim. Acta* **1986**, *121*, 175. (d) Bartlett, K. L.; Goldberg, K.; Thatcher Borden, W. *Organometallics* **2001**, *20*, 2669.

(3) Frey, U.; Helm, L.; Merbach, A. E.; Romeo, R. *J. Am. Chem. Soc.* **1989**, *111*, 8161.

(4) Romeo, R. *Comments Inorg. Chem.* **1990**, *11*, 21.

lability increase in their substitution reactions, and that they tend to operate through a dissociatively activated mechanism.<sup>5</sup>

We have been interested in the last few years on the mechanisms of formation and substitution reactions of cyclometalated platinum and palladium complexes with a variety of imines.<sup>6</sup> Dimethyl sulfide substitution by phosphines on cyclometalated Pt(IV) complexes of the type shown in eq 1 have already been studied.<sup>5a</sup>

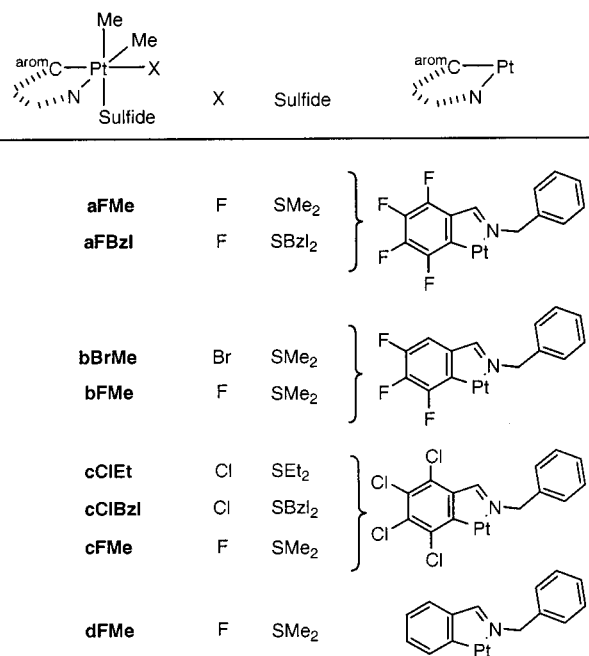


The results indicated the operation of a substitution mechanism involving the limiting dissociation of the leaving  $\text{SMe}_2$  ligand, followed by the rapid entering of the substituting phosphine. Although the discrimination factor between the back entrance of the leaving sulfide ligand and that of the different phosphines studied was not important, despite the large electronic and steric differences chosen, thermal activation parameters were found to be consistent with the proposed mechanism. Nevertheless, a certain electronic tuning related to the nature of the halogen, X, ligand and the presence of electron-withdrawing substituents affecting the aromatic metalated carbon has been found for the activation entropy values. Namely, a lesser degree of dissociation to go to the transition state was observed when the cyclometalated compound contained a maximum of electron-withdrawing elements.<sup>5a</sup>

Along the same line, we decided to follow our studies by introducing even stronger electron-withdrawing substituents affecting the aromatic metalated carbon donor, as well as increasing the electronegativity of the halo ligand. We present in this paper the study of the sulfide substitution reactions of the fluoro and fluoro-substituted complexes shown in Chart 1 by a variety of phosphines, in different solvents and at varying temperatures, to establish a possible associative drifting in the reaction mechanism.

For this purpose a number of new cyclometalated compounds have been prepared and characterized to vary, as smoothly as possible, the electronic and steric characteristics of the reactants; their full low-temperature proton and NOE NMR characterization has been especially important for this purpose. The results obtained have indicated that this type of tuning is possible, and the first associatively activated substitution process on organometallic Pt(IV) compounds has been established.<sup>7</sup> Furthermore, our results indicate that, while electronic tuning becomes a *condition sine qua non* for important shifts in the associative/dissociative mechanistic

Chart 1



continuum,<sup>4</sup> steric effects are responsible for the smaller shifts observed in these and other systems.<sup>8</sup> The operation of hydrogen bonding for these systems has also been proved, indicating that their existence in the transition state for the reactions studied leads to a decrease in the entropy,<sup>9</sup> even when dissociation of the leaving ligand in the transition state is clear.

## Results and Discussion

**Products.** Compound **aFMe** has been prepared as described in the literature.<sup>6a</sup> Complex **bBrMe** has been prepared by the well-established method of oxidative addition of  $\text{MeBr}$  on the cyclometalated Pt(II) compound  $[\text{Pt}(\text{Me})(4,5,6\text{-F}_3\text{C}_5\text{CHCHNCH}_2\text{Ph})(\text{SMe}_2)]$ .<sup>10</sup> Complexes with  $\text{SEt}_2$  and  $\text{SBzl}_2$  ligands, **cClEt**, **cClBzl**, and **aFBzl**, have been obtained via substitution of the  $\text{SMe}_2$  ligand in acetone solution of the corresponding dimethyl sulfide complexes.<sup>11</sup> Complexes **bFMe**, **cFMe**, and **dFMe** have been prepared via reaction of the corresponding bromo or chloro derivatives with  $\text{AgF}$  in acetone solution to produce the final desired compounds.<sup>12</sup> Reaction of the dimethyl sulfide derivatives with the corresponding phosphine ligands in acetone solution produced the expected complexes,<sup>11</sup> which have been characterized by their  $^1\text{H}$  and  $^{31}\text{P}$  NMR spectra.

For the sulfide complexes, in most of the cases the  $^1\text{H}$  NMR signal of the alkyl protons from the sulfide is rather broad. An increase of the temperature to the maximum

(5) (a) Bernhardt, P. V.; Gallego, C.; Martinez, M. *Organometallics* **2000**, *19*, 4862. (b) Nakayama, K.; Kondo, Y.; Ishihara, K. *Can. J. Chem.* **1998**, *76*, 62. (c) Kondo, Y.; Oda, Y.; Ishihara, K. *Int. J. Chem. Kinet.* **1998**, *30*, 523.

(6) (a) Crespo, M.; Martinez, M.; Sales, J. *Organometallics* **1993**, *12*, 4297. (b) Crespo, M.; Martinez, M.; de Pablo, E. *J. Chem. Soc., Dalton Trans.* **1997**, 1321. (c) Gómez, M.; Granell, J.; Martinez, M. *J. Chem. Soc., Dalton Trans.* **1998**, 37. (d) Gómez, M.; Granell, J.; Martinez, M. *Organometallics* **1997**, *16*, 2539.

(7) Crumpton, D. W.; Goldberg, K. I. *J. Am. Chem. Soc.* **2000**, *122*, 962.

(8) González, G.; Martinez, M.; Rodriguez, E. *J. Chem. Soc., Dalton Trans.* **1995**, 891.

(9) (a) Benzo, F.; Bernhardt, P. V.; González, G.; Martinez, M.; Sienra, B. *J. Chem. Soc., Dalton Trans.* **1999**, 3973. (b) Martinez, M.; Pitarque, M. A.; van Eldik, R. *Inorg. Chim. Acta* **1997**, *256*, 51.

(10) Crespo, M.; Font-Bardía, M.; Solans, X. *Polyhedron* **2002**, *21*, 105.

(11) Crespo, M.; Martinez, M.; Sales, J.; Solans, X.; Font-Bardía, M. *Organometallics* **1992**, *11*, 1288.

(12) Fraser, S. L.; Antipin, M. Y.; Khroustalyov, V. N.; Grushin, V. V. *J. Am. Chem. Soc.* **1997**, *119*, 4769.

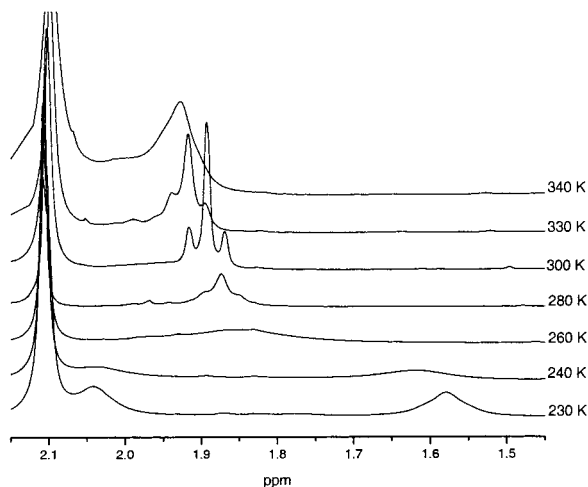


**Figure 1.** Variable-temperature  $^1\text{H}$  NMR in the  $\text{SMe}_2$  region for the compound **dFMe** in the presence of free dimethyl sulfide ligand.

possible for the solvents used indicated the presence of a dynamic process with free sulfide, as expected for the rate constant found for its interchange (see below). 2D  $^1\text{H}$  NOESY experiments have already indicated that this process includes the interchange of the two platinum-bonded methyl groups via a turnstile twist process that stops when the less labile phosphine derivative is considered or when the temperature is decreased.<sup>5a,13</sup> Nevertheless, even when the temperature is decreased, no better  $^1\text{H}$  NMR signals are obtained; Figure 1 is representative for the spectra obtained for these situations.

The spectrum measured at 230 K clearly indicates the nonequivalence of the two sulfide methyl groups for the **dFMe** system; hindered rotation and/or sulfur atom inversion of the Pt–S bond have to be held responsible for this fact even at this relatively high temperature.<sup>14</sup> This effect is also present at room temperature for the **aFBzl** and **cCIBzl** complexes. Despite the fact that the alkyl protons of each of the Bzl groups are nonequivalent at 298 K, the two Bzl groups are equivalent (two doublets at  $\delta_a = 3.79$  and  $\delta_b = 3.94$  ppm,  $J(\text{Ha}–\text{Hb}) = 14$  Hz,  $^2J(\text{Pt}–\text{Ha}) = 11.3$  Hz,  $^2J(\text{Pt}–\text{Hb}) = 7.8$  Hz, for **cCIBzl** and at  $\delta_a = 3.67$  and  $\delta_b = 3.83$  ppm,  $J(\text{Ha}–\text{Hb}) = 14$  Hz,  $^2J(\text{Pt}–\text{Ha}) = 9.2$  Hz,  $^2J(\text{Pt}–\text{Hb}) = 7.6$  Hz, for **aFBzl**). Nevertheless, on decreasing the temperature the signals become four, not completely resolved, doublets, indicating the stopping of the Pt–S bond motion. The nonequivalence of the four protons, and the presence of  $^2J(\text{Pt}–\text{H})$ , does not allow for any further estimation of the higher coalescence temperature expected for the hindered rotation in these complexes. Low-temperature (210–235 K) NOE measurements have been carried out for the  $\text{SMe}_2$  complexes to establish the geometric ligand distribution around the Pt(IV) center (Chart 2).<sup>11</sup>

The NOE effect was observed between the  $\text{Me}_{\text{eq}}$  and  $\text{SMe}_2$  resonances, whereas no effect was observed between  $\text{Me}_{\text{ax}}$

**Chart 2**

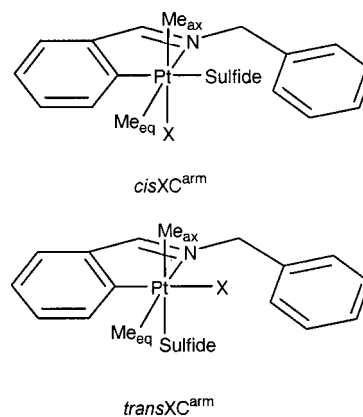


**Table 1.** Crystal Data and Relevant Bond Angles and Distances for the Crystal Structure of Compound **cCIBzl**

		bonds	length/Å	angle/deg
space group	<i>P</i> 21 (no. 4)	Pt1–S1	2.482(2)	
empirical formula	$\text{C}_{30}\text{H}_{28}\text{Cl}_5\text{NPtS}$	Pt1–Cl1	2.403(2)	
		Pt1–N1	2.154(5)	
<i>a</i> , Å	10.818(1)	Pt1–C1	2.079(6)	
<i>b</i> , Å	12.224(1)	Pt1–C2	2.060(6)	
<i>c</i> , Å	12.162(2)	Pt1–C3	2.037(5)	
$\beta$ , deg	110.44(1)	Cl1–Pt1–S1		94.5(2)
<i>V</i> , Å <sup>3</sup>	1507.1(3)	C3–Pt1–S1		96.5(2)
$\rho_{\text{calcd}}$ , g cm <sup>−3</sup>	1.877	C1–Pt1–S1		94.5(2)
fw	806.93	N1–Pt1–S1		90.9(1)
<i>Z</i>	2	C1–Pt1–Cl1		86.8(2)
$\mu$ , cm <sup>−1</sup>	5.189	S1–Pt1–C2		92.3(1)
temp, K	296	Cl1–Pt1–C2		176.5(2)
$\lambda$ , Å	0.10377	C3–Pt1–C2		90.9(2)
<i>N</i>	2967	C1–Pt1–C2		86.5(2)
$N_o$ ( $F_o > 2\sigma$ )	2657	N1–Pt1–C2		86.6(3)
$2\theta_{\text{max}}$ , deg	50	C1–Pt1–C3		88.0(2)
$R_1(F_o)$	0.0185, 0.0462	N1–Pt1–C3		101.0(3)
$wR_2(F_o^2)$				79.7(2)
( $I > 2\sigma(I)$ )				

and  $\text{SMe}_2$ , indicating that the *trans*- $\text{XC}^{\text{arm}}$  geometrical isomer is the one present in solution under these conditions, as already found for the series of sulfide and phosphine derivatives whose structure has been established by X-ray crystallography.<sup>5a,11</sup> In this respect, the X-ray crystal structure determination of compound **cCIBzl** has been carried out (Table 1, Figure 2).

The structure (Tables S1–S6, Supporting Information) indicates the preference for the *trans*- $\text{XC}^{\text{arm}}$  arrangement in these complexes, as expected especially for this bulky sulfide ligand. The view of the structure in Figure 2 clearly shows the hindrance around the chloro ligand does not allow for a possible *cis*- $\text{XC}^{\text{arm}}$  arrangement of the complex. Furthermore, the stacking of the C3–C8 and C25–C30 rings establishes a frozen rotational position of the sulfide ligand very different from that observed for the  $\text{SMe}_2$  analogue,<sup>5a</sup> where the sulfide substituents are positioned away from the metalated ring of the complex. The octahedral coordination angles, as a whole, are more distorted, as expected for the bulkiness of the coordinated  $\text{SBzl}_2$  ligand that forces the angles further away from  $90^\circ$ , than those determined for the dimethyl sulfide analogue. Those two facts, involving the S–C1–Cl1 facial arrangement, produce a much more open structure than expected for the increase in the bulkiness of the ligand. Even more interesting is the fact that the Pt–Me, Pt– $\text{aromC}$ , and

(13) (a) Ugi, I.; Ramirez, F.; Marquarding, D.; Klusacek, H.; Gokel, G.; Guillespie, P. *Angew. Chem., Int. Ed. Engl.* **1970**, *9*, 703. (b) Casares, J. A.; Espinet, P. *Inorg. Chem.* **1997**, *36*, 5428.

(14) Méndez, N. Q.; Arif, A. M.; Gladysz, J. A. *Organometallics* **1991**, *10*, 2199.

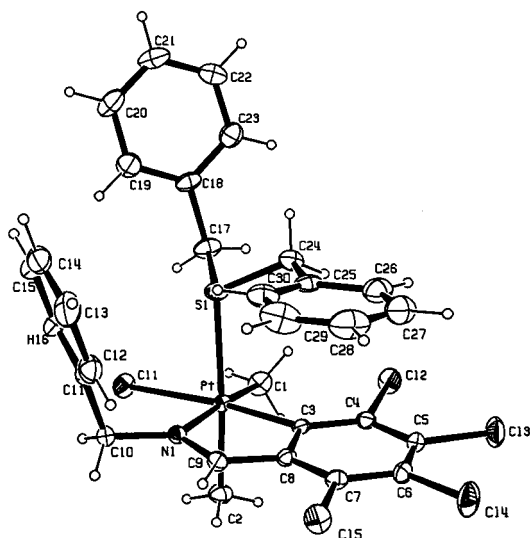
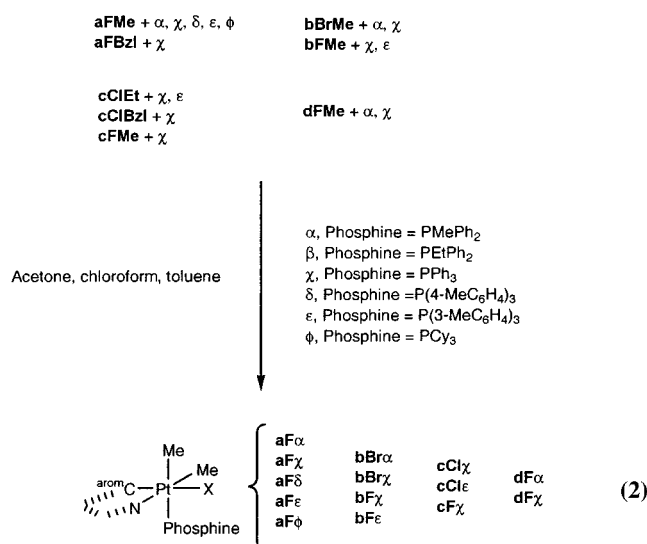


**Figure 2.** View of the complex **cClBzl**. Ellipsoids indicate 20% probability.

Pt–N bond distances do not become affected by the changes in the sulfide ligand, despite the fact that not only the Pt–S bond distance increases by 0.013 Å but also the corresponding Pt–Cl distance increases by 0.015 Å on going from the **cClMe**<sup>5a,15</sup> to the **cClBzl** complex. Again, this results in a significant decrease in the steric hindrance of the S–C1–C11 octahedral face, leaving it much more open.

**Mechanism.** The substitution reactions studied are those summarized in eq 2 and have been monitored via electronic spectroscopy. The monitoring of these reactions via <sup>31</sup>P and <sup>1</sup>H NMR indicated that the reaction is clean, and that the products formed are the expected (see above). No equilibrium has been detected via NMR spectroscopy for any of the systems studied under the kinetic conditions used, even at high added sulfide concentrations, and reverse rate constants have not been considered as in the previous systems studied.<sup>5a</sup>



Observed pseudo-first-order rate constants were found independent of the concentration of the platinum complex and dependent on the concentration of the entering ligand.

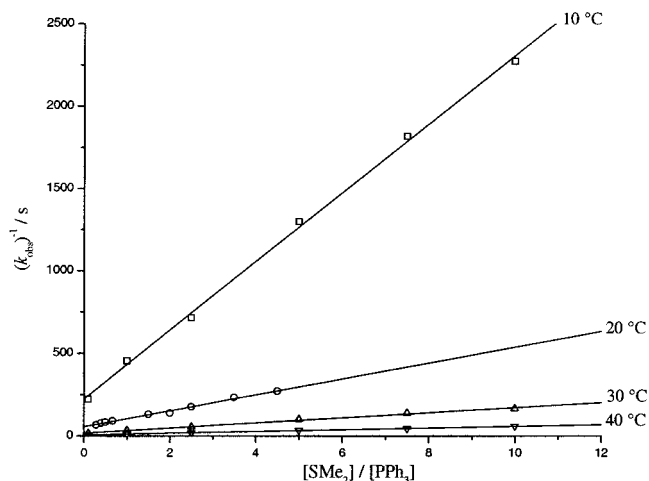


**Figure 3.**  $1/k_{\text{obs}}$  as a function of  $[\text{PPh}_3]/[\text{SMe}_2]$  for the **bFMe** plus  $\chi$  system studied in acetone solution.

For most of the systems studied, an inverse dependence on the leaving sulfide ligand concentration has also been found. This is not the case for reaction of compound **aFMe** with phosphines  $\alpha$ ,  $\chi$ ,  $\delta$ , and  $\epsilon$ , while for the bulky  $\text{PCy}_3$ ,  $\phi$ , the situation reverses to the  $[\text{phosphine}]/[\text{sulfide}]$  dependence. Figures 3 and 4 show the typical concentration dependence behavior for these systems.

In view of the  $[\text{sulfide}]/[\text{phosphine}]$  dependence of  $(k_{\text{obs}})^{-1}$  shown in Figure 3, and previously published work, the reaction mechanism and rate law depicted in Scheme 1 and eq 3 were used to fit the data for the systems indicated.

$$k_{\text{obs}} = \frac{k_1 k_2 [\text{phosphine}]}{k_{-1} [\text{sulfide}] + k_2 [\text{phosphine}]}$$

$$k_{\text{obs}} = \frac{k_1 k_2 ([\text{phosphine}]/[\text{sulfide}])}{k_{-1} + k_2 ([\text{phosphine}]/[\text{sulfide}])} \quad (3)$$

$$1/k_{\text{obs}} = \{1/k_1\} + \{k_{-1}/(k_1 k_2)\}([\text{sulfide}]/[\text{phosphine}])$$

From the temperature dependence of the rate constants derived from intercepts of the double inverse plot of eq 3, and by standard Eyring plots, thermal activation parameters can be derived. Table 2 collects all the relevant kinetic and activation parameters for the systems studied showing this behavior, together with relevant literature data for comparison. In the same table it is indicated when no differences in Eyring plots are observed on changing the phosphine entering ligand and/or solvent used for the substitution reactions on the same substrate (Figure S1, Supporting Information). In this case a combined fitting has also been used for the derivation of the thermal activation parameters.<sup>5a</sup>

As stated before, for the **aFMe** plus  $\alpha$ ,  $\chi$ ,  $\delta$ , or  $\epsilon$  substitution reactions, no inhibition of the reaction rate is obtained with increasing leaving ligand concentration in the reaction medium. Consequently, the reaction mechanism and rate law

(15) Compounds **cClMe** and **dBrMe** have not been studied in this work, but in ref 5a, and are not included in Chart 1; nevertheless, the nomenclature established there has been maintained in the text.

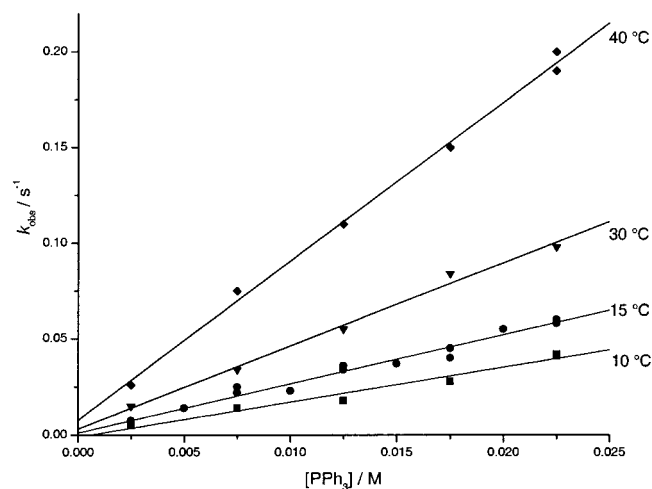
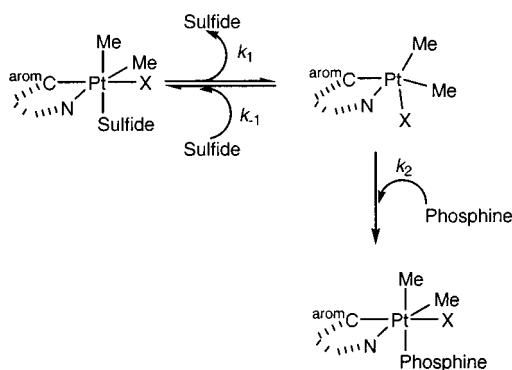


**Figure 4.** Observed rate constants,  $k_{\text{obs}}$ , as a function of phosphine concentration for the **aFMe** plus  $\chi$  system studied in acetone solution. Multiple points with the same  $[\text{PPh}_3]$  indicate different values of added  $[\text{SMe}_2]$ .

### Scheme 1



indicated in Scheme 2 and eq 4 have been applied for the systems mentioned.

$$k_{\text{obs}} = k_2[\text{phosphine}] \quad (4)$$

Table 3 collects all the determined kinetic parameters derived for these systems together with the corresponding thermal activation parameters obtained from their temperature dependence. Significant data obtained for the limiting inhibited process (Scheme 1, eq 3) for the same complex are also included for comparison.

For the substitution reactions of the systems following Scheme 1, it is clear that a limiting dissociative mechanism is operating for the process.<sup>16</sup> This fact has already been established for a variety of complexes and substitution reactions of the same type.<sup>5</sup> The general trend observed in Table 2 is in agreement with a dominant steric tuning of the mechanism proposed in Scheme 1. The Lewis donor basicity of the entering ligands does not seem to play an important role.<sup>17</sup> The activation parameters related to the  $\{k_1/k_{-1}\}k_2$  term, derived from the slopes of eq 3 (Table S7, Supporting

**Table 2.** Summary of the Relevant Kinetic (Extrapolated from Eyring Plots at 298 K) and Activation Parameters Derived from the Rate Law Indicated in Eq 3 for the Systems Studied and Literature Data

complex	entering ligand	solvent	$10^2 k_1^{298}/\text{s}^{-1}$	$\Delta H_1^\ddagger/\text{kJ mol}^{-1}$	$\Delta S_1^\ddagger/\text{J K}^{-1} \text{mol}^{-1}$	$k_{-1}/k_2^a$
<b>aFMe</b>	$\phi$	acetone	1.2	$75 \pm 4$	$-33 \pm 14$	1.3
		toluene	1.7	$78 \pm 3$	$-17 \pm 10$	1.7
<b>aFBzl</b>	$\chi$	acetone	14	$51 \pm 3$	$-90 \pm 12$	0.40
		toluene	19	$63 \pm 4$	$-49 \pm 14$	0.29
<b>bBrMe</b>	$\alpha$	acetone	5.0	$92 \pm 6$	$39 \pm 19$	1.2
		acetone	4.2	$98 \pm 4$	$57 \pm 14$	1.8
<i>e</i>			<b>4.7</b>	<b>99 ± 4</b>	<b>48 ± 12</b>	
<b>bFMe</b>	$\chi$	acetone	3.0	$84 \pm 3$	$6 \pm 10$	0.86
		acetone	3.1	$84 \pm 2$	$5 \pm 7$	0.88
		toluene <sup>b</sup>	3.0			1.0
<i>e</i>			<b>3.0</b>	<b>85 ± 2</b>	<b>9 ± 8</b>	
<b>cClMe<sup>c</sup></b>	$\chi$	acetone	3.6	$96 \pm 4$	$48 \pm 12$	0.97
		acetone	3.6	$88 \pm 4$	$22 \pm 14$	1.1
		chloroform	4.6	$89 \pm 2$	$48 \pm 12$	1.1
		chloroform	5.1	$89 \pm 1$	$27 \pm 5$	1.6
<i>e</i>			<b>4.0</b>	<b>91 ± 3</b>	<b>31 ± 10</b>	
<b>cClEt</b>	$\chi$	acetone	20	$52 \pm 6$	$-85 \pm 19$	0.67
		acetone	25	$65 \pm 5$	$-51 \pm 15$	0.96
<i>e</i>			<b>21</b>	<b>57 ± 4</b>	<b>-69 ± 12</b>	
<b>cClBzl</b>	$\chi$	toluene	52	$88 \pm 6$	$42 \pm 19$	1.3
		acetone	52	$55 \pm 3$	$-68 \pm 11$	0.91
$\chi$	chloroform		53	$59 \pm 4$	$-56 \pm 15$	1.2
			53	$57 \pm 2$	$-62 \pm 8$	
<i>e</i>			<b>53</b>	<b>57 ± 2</b>	<b>-62 ± 8</b>	
$\chi$	toluene		89	$76 \pm 1$	$9 \pm 5$	1.8
		toluene <sup>d</sup>				1.8
<i>e</i>			<b>91</b>	<b>78 ± 2</b>	<b>15 ± 7</b>	
<b>cFMe</b>	$\chi$	acetone	2.5	$82 \pm 6$	$-2 \pm 10$	0.57
		toluene	3.5	$80 \pm 3$	$-7 \pm 9$	0.83
		toluene <sup>d</sup>				0.77
<i>e</i>			<b>2.9</b>	<b>81 ± 4</b>	<b>-4 ± 15</b>	
<b>dFMe</b>	$\alpha$	acetone	4.3	$72 \pm 7$	$-32 \pm 23$	0.51
		acetone	3.3	$69 \pm 4$	$-44 \pm 13$	0.96
		toluene <sup>d</sup>				0.89
<i>e</i>			<b>3.7</b>	<b>70 ± 4</b>	<b>-39 ± 12</b>	

<sup>a</sup> Average for the temperatures studied. <sup>b</sup> Only runs at 25 and 35 °C have been carried out. <sup>c</sup> From ref 5a. <sup>d</sup> Only runs at 15 and 35 °C have been carried out. <sup>e</sup> Combined fitting for all  $k_1$  values for the substitutions by different phosphines and/or solvents (see the text).

### Scheme 2

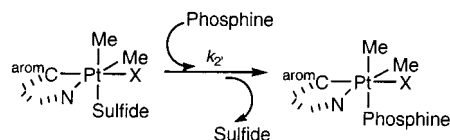


**Table 3.** Summary of the Kinetic and Activation Parameters Derived from the Rate Law Indicated in Eq 4 for the **aFMe** System Studied

entering ligand	solvent	$k_2^{298}/\text{M}^{-1} \text{s}^{-1}$	$\Delta H_2^\ddagger/\text{kJ mol}^{-1}$	$\Delta S_2^\ddagger/\text{J K}^{-1} \text{mol}^{-1}$	$10^{-2}\{k_2/k_1\}^a/\text{M}$
$\alpha$	acetone	60	$28 \pm 1$	$-120 \pm 2$	50
$\chi$	acetone	3.9	$33 \pm 3$	$-125 \pm 10$	3.2
	toluene	6.8	$41 \pm 2$	$-93 \pm 8$	4.0
$\delta$	acetone	6.2	$33 \pm 1$	$-120 \pm 1$	5.1
	toluene	11	$42 \pm 1$	$-88 \pm 1$	6.3
$\epsilon$	acetone	3.7	$38 \pm 2$	$-107 \pm 6$	4.0
	toluene	6.5	$44 \pm 2$	$-83 \pm 6$	3.1

<sup>a</sup> Average for the temperatures studied.  $k_1$  derived from Table 2 data.

Information), are not reliable separately given the fact that they are composites. Nevertheless, a  $\Delta H^\ddagger/\Delta S^\ddagger$  compensation plot (Figure 5)<sup>18</sup> for all the systems studied, including those from ref 5a, indicates that there is clear a difference between the reactions of the  $\text{SMe}_2$  and the  $\text{SEt}_2$  or  $\text{SBzl}_2$  ligand

(16) (a) Tobe, M. L.; Burgess, J. *Inorganic Reaction Mechanisms*; Longman: Harlow, U.K., 1999. (b) Espenson, J. H. *Chemical Kinetics and Reaction Mechanisms*, 2nd ed.; McGraw-Hill: New York, 1995. (17) (a) Chen, L.; Poe, A. J. *Coord. Chem. Rev.* **1995**, *143*, 265. (b) Goodfellow, R. J.; Goggin, P. L.; Duddell, D. A. *J. Chem. Soc. A* **1968**, 504.

(18) Liu, L.; Guo, Q.-X. *Chem. Rev.* **2001**, *101*, 673.

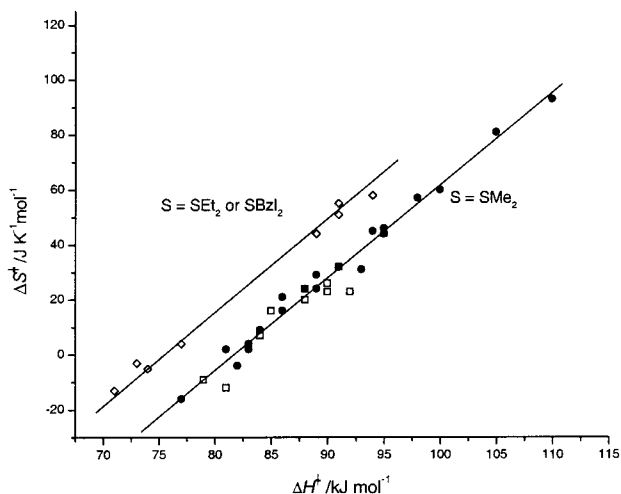


**Figure 5.** Compensation plot for the thermal activation parameters related to the  $\{k_1/k_{-1}\}k_2$  composite term of eq 3. Full circles indicate data from ref 5a.

complexes. A difference of ca.  $6.5 \text{ kJ mol}^{-1}$  in the value of  $\Delta G^\ddagger$  for both sets of systems is evident, which has to be related solely to the more facile dissociation of the bulkier sulfide ligands ( $\Delta G_1^\circ$ ). Given the fact that the  $\text{SEt}_2$  ligand is the best  $\sigma$ -donor,<sup>17</sup> no electronic influences from the leaving ligand seem to be present. If this compensation translates to separated isokinetic relationships for the two sets of systems, a clear reference to the Pt–S bond breaking process is established.<sup>19</sup>

Discussion of the available kinetic and thermal activation parameters related to process 1 in Scheme 1 ( $k_1$ ) seems much more straightforward. Activation enthalpies are expected to be high, while their activation entropies should be clearly positive.<sup>5a</sup> The effects on the values of  $k_1$  of the size of the leaving ligand are clearly evident in the data of the **cCIME**, **cCIET**, and **cCIBzl** plus  $\chi$  systems in acetone solution collected in Table 2; an increase of more than 1 order of magnitude is observed. The nature of the halo ligand provides the expected changes also; both going from **bBrMe** to **bFMe** and going from **cCIME** to **cFMe** produce a decrease in the value of  $k_1$  that is not as important as in the previous instance. Changes in the substituents of the metalated ring do not seem to produce measurable changes, as seen on comparing **bFMe**, **cFMe**, and **dFMe** plus  $\chi$  data; only when the fully fluorinated metallacycle is introduced (from **bFMe** to **aFMe**) is a measurable difference apparent. Changes in the entering ligand do not produce any differences in the values derived, which allows the thermal activation parameters to be calculated from combined plots (Figure S1, Supporting Information).<sup>5a</sup> The fact that the activation entropy varies from values clearly positive (as expected) to clearly negative, given the dissociative character of the substitution process, is surprising; activation enthalpy values vary accordingly from large to small values. While the largest negative entropies are present for systems with the bulkier leaving ligands and in solution of the more polar solvents, the complexes with fluoro ligands produce values closer to zero; for the remain-

ing systems the activation entropy values are in the expected positive range.<sup>5a</sup> Especially revealing is the plot of Figure S2 (Supporting Information), where the difference of ca.  $2 \text{ kJ mol}^{-1}$  in the value of the energy of activation at 298 K (Table 2) is indicative of the entropic control of the more facile decoordination of  $\text{SBzl}_2$ .

Anyway, the zero or negative values of the activation entropies need to be explained. The fact that the  $\text{CH}_2$  groups of the  $\text{SEt}_2$  and  $\text{SBzl}_2$  ligands are more prone to hydrogen bonding than the methyl groups of the dimethyl sulfide ligand<sup>17</sup> and the presence of fluoro ligands/substituents could be held responsible for this observation. If solvent-assisted hydrogen bonding is established between the sulfide and the fluoro ligand of the complex, Pt–S bond breaking should not produce a more disordered transition state for the dissociation of the ligand. On the contrary, the leaving sulfide would be poorly connected to both the Pt(IV) center and the F ligand/substituent, producing a highly ordered dissociative transition state as found for other systems.<sup>9</sup> This effect should be more evident for complexes with ligands more prone to form hydrogen bonding, as  $\text{SEt}_2$  and  $\text{SBzl}_2$  are. Solvent polarity should also favor this effect. When the reactions are carried out in toluene, the lesser importance of this effect is reflected in the values of the activation entropies that enable a faster substitution process, as observed in the values collected in Table 2. From these data it is clear that, while the effect of changing from  $\text{X} = \text{Br}$  or  $\text{Cl}$  to  $\text{X} = \text{F}$  or from  $\text{S} = \text{SMe}_2$  to  $\text{S} = \text{SEt}_2$  or  $\text{SBzl}_2$  is huge, changing the substituents on the ring that contains the metalated carbon does not seem to have such an important effect.

Finally, with reference to the discrimination factor  $k_{-1}/k_2$  the results indicated in Table 2 are less clear-cut when compared with the values obtained for previously published studies.<sup>5a</sup> Although the changes in the leaving ligand should produce clear differences, the discrimination factor for a given entering phosphine ligand seems to be independent of the leaving sulfide group, as can be seen when the set of complexes **cCIME**, **cCIET**, and **cCIBzl** are considered. Probably the above-mentioned hydrogen bonding in the transition state facilitates the back-entering of the sulfide ligand in such a way that any discrimination is compensated.

As a whole, it seems that hydrogen bonding plays a key role in the substitution mechanism operating for this type of complex; nevertheless, a certain degree of electronic tuning had also been established with reference to the presence of electron-withdrawing substituents in the metalated ring and the electronegativity of the halo ligand present in the platinum complex.<sup>5a</sup> In this respect, when compound **aFMe** is considered, but the entering ligands are set to have smaller cone angles, the substitution behavior changes dramatically, and the kinetic and activation parameter values collected in Table 3 can be derived according to Scheme 2 and eq 4. From these values, it is clear that the reaction mechanism becomes associatively activated, with small values of the enthalpies of activation and large negative activation entropies; furthermore, these parameters depend on the solvent used as expected. The trend is that expected for an associatively activated sterically controlled substitution mech-

(19) Larson, R. *React. Kinet. Catal. Lett.* **1999**, *68*, 115.

anism.  $\Delta H_2^\ddagger$  is larger for the bulkier phosphines, while the value of  $\Delta S_2^\ddagger$  is kept constant for all the reactions studied. The apparent misbehavior of the trend in  $k_2$  for the  $\chi$ ,  $\delta$ , and  $\epsilon$  entering phosphines can be easily related to the important changes in their Lewis basicity. It has been proved that the values of the stereoelectronic factors of phosphines are not linear with respect to the classical cone angle and electronic parameters; that is, the relative weight of steric and electronic factors is not common to all the phosphine ligands.<sup>20</sup> The reactions carried out in toluene have larger values of  $\Delta H_2^\ddagger$ , while those of  $\Delta S_2^\ddagger$  are less negative; if we accept that hydrogen bonding also plays a part in these reactions, the processes carried out in acetone should favor the interaction between the leaving sulfide and the fluorine atoms in the complex, producing a more ordered transition state with a lesser energy demand to be formed. Comparison of the dissociative and associative activation rate constants produces ratio figures (Table 3) that indicate that, for these systems, the reactions through the associative path are preferred by a factor of 2–3 orders of magnitude, which practically does not give room for the dissociative mechanism to be detected. Kinetic experiments run with [phosphine]/[sulfide] held constant, but with increasing phosphine concentration, have been carried out to check the possible existence of this  $k_2$  path for the systems dissociatively activated described before. That is, combination of eqs 3 and 4 has been tried; no significant increase from the determined  $k_1$  values has been obtained, indicating that the availability of reaction path  $k_2$  is limited to the Pt(IV) center with highly electron-withdrawing ligands and smaller leaving and entering ligands.<sup>21</sup> A possible explanation of the associativeness observed can easily be related to the fact that the presence of highly electron-withdrawing substituents produce a Pt(IV) much more acidic, which would make both make the Pt–S bond stronger and the association with an entering nucleophile more facile. In this respect, 2D NOESY NMR experiments indicated that, for **aFMe**, the exchange of the two methyl groups due to the interchange of the dimethyl sulfide ligand, observed for all the other complexes, does not take place under the experimental conditions. The reason this effect is only apparent on the substitution reactions on **aFMe** is not clear, but the presence of a perfluorinated metalated ring *plus* a fluoride substituent seems to do the trick.<sup>22</sup>

Summarizing, the first associatively activated substitution process on an organometallic Pt(IV) complex has been established. The type of activation of the process can be tuned via both the acidity induced on the Pt(IV) center by highly

electronegative ligands and the presence of tight outer-sphere (noncoordination) interactions between the coordinated leaving and/or entering substituting ligands and the cyclometalated complex. Hydrogen bonding seems to play a crucial role in many of these reactions, and the existence of solvent-assisted dead-end complexes in some of the cases produces a set of thermal activation parameters that does not seem to fit with the established dissociative mechanism found in some of the cases studied. The determined X-ray crystal structure of the **cCIBzl** compound agrees very well with these outer-sphere interactions, the compound showing a geometrical arrangement that should not be the favored one in the dynamic solution media.

## Experimental Section

**Instruments.** <sup>1</sup>H NMR spectra were recorded with Varian XL-200, Varian XL-300, Bruker 250 DRX, Bruker 500 DRX, and Bruker 500 DMX spectrometers, while <sup>31</sup>P{<sup>1</sup>H} and <sup>195</sup>Pt NMR spectra were obtained by using a Bruker 250 DRX (101.25 and 53.5 MHz, respectively) spectrometer. Chemical shifts (ppm) were measured relative to SiMe<sub>4</sub> for <sup>1</sup>H and to 85% H<sub>3</sub>PO<sub>4</sub> for <sup>31</sup>P spectra; the solvent used was acetone-*d*<sub>6</sub>. All spectra were obtained at the Unitat de RMN d'Alt Camp de la Universitat de Barcelona and the Servei de Resonància Magnètica Nuclear de la Universitat Autònoma de Barcelona.

**Products.** All the phosphine ligands used in this study were used as commercially available; solvents were distilled and kept under N<sub>2</sub>. Complexes **aFMe**, **cCIME**, and **dBrMe** were prepared according to the established literature procedures.<sup>6a,11</sup> The complex **bBrMe** was prepared by reaction of 0.3 g of [Pt(Me)(4,5,6-F<sub>3</sub>C<sub>5</sub>CHCHN(CH<sub>2</sub>Ph)(SMe<sub>2</sub>)]<sup>12</sup> in 50 cm<sup>3</sup> of acetone solution with 1–2 cm<sup>3</sup> of BrMe. After being stirred for 2 h at room temperature the solution was taken to dryness and the solid washed with hexane, yield 79% Anal. Calcd for PtC<sub>18</sub>H<sub>21</sub>NBrF<sub>3</sub>S, **bBrMe**: N, 2.28; C, 35.1; H, 3.44. Found: N, 2.45; C, 35.5; H, 3.49. Compounds **aFBzl**, **cCIET**, and **cCIBzl** were prepared by dissolving 0.3 g of the corresponding SMe<sub>2</sub> derivatives in 30 cm<sup>3</sup> of acetone and further addition of a 4-fold excess of the corresponding substituting sulfide. After being stirred at 40 °C for 24 h, the solutions were taken to dryness and the solids washed repetitively with hexane, yields 50–70%. Compounds **bFMe**, **cFMe**, and **dFMe** were prepared by dissolving 0.25 g of the corresponding chloro or bromo derivatives (**bBrMe**, **cCIME**, **dBrMe**)<sup>15</sup> in 50 cm<sup>3</sup> of acetone and addition of a stoichiometric amount of AgF in 10 cm<sup>3</sup> of methanol. Stirring for 5 min produced the complete precipitation of the corresponding silver halides, which were filtered. Concentration of the solution to dryness produced the desired compounds in 60–75% yield. If necessary, all products can be further purified by recrystallization in acetone/hexane solution. All new complexes were characterized by <sup>1</sup>H NMR spectra. Table S9 (Supporting Information) collects all relevant data for the complexes prepared.

For the phosphine-substituted derivatives the standard published procedure<sup>11</sup> was also applied; characterization of the complexes was achieved via <sup>31</sup>P and <sup>1</sup>H NMR spectra. Table 4 collects all the characterization NMR data from the new phosphine-substituted compounds.

**Crystallography.** Good-quality X-ray crystals from the compound **cCIBzl** were obtained by cooling a concentrated acetone solution of the complex in a refrigerator for extended periods. Intensity data for the compounds were measured on an Enraf-Nonius CAD4 four-circle diffractometer using graphite-monochromated Mo

(20) (a) Martinez, M.; Muller, G. *J. Chem. Soc., Dalton Trans.* **1989**, 1669. (b) Fernandez, A. L.; Lee, T. Y.; Reyes, C.; Prock, A.; Giering, W. P.; Haar, C. M.; Nolan, S. P. *J. Chem. Soc., Perkin Trans. 2* **1999**, 2631.

(21) For experiments on the **aFBzl** plus  $\chi$  system at [PPh<sub>3</sub>]/[SBzl<sub>2</sub>] = 1 with triphenylphosphine concentration varying from 0.015 to 0.045 M,  $k_{\text{obs}}$  changes from 0.073 to 0.080 s<sup>-1</sup> (20 °C) or from 0.33 to 0.38 s<sup>-1</sup> (40 °C), which does not seem a large enough reliable difference to be considered, taking into account the important changes in the solution medium.

(22) Reaction of **aFMe** with LiBr in acetone solution produced the expected **aBrMe**, which behaves as the rest of the complexes studied with respect to its SMe<sub>2</sub> by PPh<sub>3</sub> substitution.

K $\alpha$  radiation ( $\lambda$  0.71073 Å) in the  $\omega/2\theta$  scan mode. Lattice dimensions were determined by a least-squares fit of the setting parameters of 25 independent reflections. Data reduction and empirical absorption corrections were performed with the XTAL package.<sup>23</sup> Structures were solved by heavy-atom methods with SHELXS-86<sup>24</sup> and refined by full-matrix least-squares analysis with SHELXL97.<sup>25</sup> All non-H atoms were refined with anisotropic thermal parameters. Crystallographic data and selected bond lengths appear in Table 1 (Tables S1–S6, Supporting Information). The atomic nomenclature is defined in Figure 1, drawn with the graphics program PLATON.<sup>26</sup>

**NOE Experiments.** NMR experiments were carried out on a 500 MHz ADVANCE spectrometer equipped with a 5 mm triple-resonance inverse broad-band probe head, a  $z$ -gradient coil controlled by a B-AFPA10 gradient unit, and a eurotherm VT-3000 temperature regulation system. Selective 1D NOESY<sup>27</sup> and selective 1D ROESY<sup>28</sup> experiments were performed using a double-pulsed field-gradient echo as a selective excitation, in which the 180° pulse has a Gaussian shape truncated to 1%. The duration of this pulse was set accordingly to the required selectivity. When selective excitation was not feasible, phase-sensitive 2D NOESY<sup>29</sup> spectra were recorded using basically the same previously described conditions. In all experiments, the number of scans was set as a function of sample concentration, and the mixing time for both NOESY and ROESY processes was set to 500 ms. The temperature of the NMR experiments also varied with each sample. In practice, the sample temperature was progressively lowered until no chemical exchange effects between methyl signals were observed.

(23) Farrugia, L. J. *J. Appl. Crystallogr.* **1999**, *32*, 837.

(24) Sheldrick, G. M. *Acta Crystallogr.* **1990**, *A46*, 467.

(25) Sheldrick, G. M. *SHELXL97, Program for Crystal Structure Determination*; University of Göttingen: Göttingen, Germany, 1997.

(26) Spek, A. L. *Acta Crystallogr.* **1990**, *A46*, C34.

(27) Stott, K.; Stonehouse, J.; Keeler, J.; Hwang, T. L.; Shaka, A. J. *J. Am. Chem. Soc.* **1995**, *117*, 4199.

(28) Gradwell, M. J.; Kogelberg, H.; Frenkiel, T. A. *J. Magn. Reson.* **1997**, *124*, 267.

**Kinetics.** The reactions were followed by UV–vis spectroscopy in the 500–330 nm range where none of the solvents absorb. Runs with  $t_{1/2} > 170$  s were recorded on an HP8452A instrument equipped with a thermostated multicell transport; runs within the 7–170 s margin were recorded on a HP8452A or a J&M TIDAS instrument and using a High-Tech SFA-11 rapid kinetics accessory. For  $t_{1/2} < 7$  s, a Durrum D-110 stopped-flow instrument connected to a J&M TIDAS spectrophotometer was used. Observed rate constants were derived from absorbance versus time traces at the wavelengths where a maximum increase and/or decrease of absorbance was observed. Table S8 (Supporting Information) collects all the obtained  $k_{\text{obs}}$  values for all the complexes studied as a function of the starting complex, entering and leaving ligands, solvent, and temperature. No dependence of the observed rate constant values on the selected wavelengths was detected, as expected for reactions where a good retention of isosbestic points is observed. The general kinetic technique is that previously described.<sup>11,30</sup> In all cases, pseudo-first-order conditions were maintained and the platinum concentration was maintained at  $(2-6) \times 10^{-4}$  M to avoid undesired decomposition reactions.

**Acknowledgment.** We acknowledge financial support for the BQU2001-3205 project from the Ministerio de Educación y Cultura.

**Supporting Information Available:** Listing of the crystal structure data for the compound **cCIBzl**, observed rate constants for the systems studied, combined  $\{k_1/k_{-1}\}k_2$  kinetic and thermal activation parameters, and relevant characterization data for the products prepared and figures showing combined Eyring plots. This material is available free of charge via the Internet at <http://pubs.acs.org>.

IC0108179

(29) Wagner, R.; Berger, S. *J. Magn. Reson., A* **1996**, *123*, 119.

(30) Martinez, M.; Pitarque, M.-A.; van Eldik, R. *J. Chem. Soc., Dalton Trans.* **1994**, 3159.